Photoelectron spectroscopy of boron-containing reactive intermediates using synchrotron radiation: BH 2 , BH, and BF

D. Mukhopadhyay, D. Schleier, I. Fischer, J.-C. Loison, C. Alcaraz, G. Garcia

PCCP

Photoelectron spectroscopy of boron-containing reactive intermediates using synchrotron radiation: BH2, BH, and BF

Journal:	*Physical Chemistry Chemical Physics*
Manuscript ID	CP-ART-11-2019-006010
Article Type:	Paper
Date Submitted by the Author:	05-Nov-2019

Complete List of Authors:	Mukhopadhyay, Deb Pratim; Universitaet Wuerzburg, Institut fuer Physikalische und Theoretische Chemie Chemie Schleier, Domenik; University of Würzburg, Institute of Physical and Theoretical Chemistry Fischer, Ingo; Universitaet Wuerzburg, Institut fuer Physikalische und Theoretische Chemie Chemie Loison, Jean-Christophe; Université Bordeaux, ISM Alcaraz, Christian; CNRS - Université Paris-Sud et Paris-Saclay, Laboratoire de Chimie Physique, UMR 8000 Garcia, Gustavo; Synchrotron SOLEIL,

PCCP

Physical Chemistry Chemical Physics

Guidelines for Reviewers

Thank you very much for agreeing to review this manuscript for *Physical Chemistry Chemical Physics (PCCP)*.

PCCP is an international journal for the publication of cutting-edge original work in physical chemistry, chemical physics and biophysical chemistry. To be suitable for publication in *PCCP*, articles must include significant innovation and/or insight into physical chemistry; this is the most important criterion that reviewers and the Editors will judge against when evaluating submissions. Further information on our scope can be found at rsc.li/pccp.

PCCP's Impact Factor is **3.567** (2018 Journal Citation Reports®)

The following manuscript has been submitted for consideration as a

PAPER

Full papers should contain original scientific work that has not been published previously. Full papers based on Communications are encouraged provided that they represent a substantial extension of the original material. There are no restrictions on the length of a paper. Authors should include a brief discussion in the Introduction that sets the context for the new work and gives their motivation for carrying out the study.

When preparing your report, please:

- Focus on the originality, importance, impact and reliability of the science. English language and grammatical errors do not need to be discussed in detail, except where it impedes scientific understanding.
- Use the journal scope and expectations to assess the manuscript's suitability for publication in *PCCP.*
- State clearly whether you think the article should be accepted or rejected and include details of how the science presented in the article corresponds to publication criteria.
- Inform the Editor if there is a conflict of interest, a significant part of the work you cannot review with confidence or if parts of the work have previously been published.

Best regards,

Professor David Rueda
Editorial Board Chair
Imperial College London, UK

Dr Anna Simpson
Executive Editor
Royal Society of Chemistry

Contact us

Please visit our reviewer hub for further details of our processes, policies and reviewer responsibilities as well as guidance on how to review, or click the links below.

What to do when you review

Reviewer responsibilities

Process & policies

Phys. Chem. Chem. Phys.

ARTICLE

Photoelectron spectroscopy of boron-containing reactive intermediates using synchrotron radiation: BH_2, BH, and BF

Received 00th January 20xx,
Accepted 00th January 20xx

DOI: 10.1039/x0xx00000x

www.rsc.org/

D.P. Mukhopadhyay,[a] D. Schleier, [a] I. Fischer [a] ,*J.-C. Loison,[b] C. Alcaraz,[c] and G. A. Garcia[d]

Mass selected slow photoelectron spectra (SPES) of three boron-containing reactive species, BH_2, BH, and BF were recorded by double imaging photoion-photoelectron coincidence spectroscopy (i²PEPICO) using synchrotron radiation. All species were generated in a flow reactor from the H-abstraction of B_2H_6 by F atoms created in a F_2 microwave discharge. The spectrum of BH_2^+ exhibits a long bending mode progression with a 970 cm^{-1} spacing due to the large geometry change from bent to linear upon ionization. Its ionization energy was determined as 8.12 ± 0.02 eV. For BH, photoionisation from both $X^1\Sigma^+$ singlet and $a^3\Pi$ triplet state was observed, permitting the experimental determination of the singlet/triplet gap (ΔE_{ST}) from the observed IE's of 9.82 eV and 8.48 eV. In addition, a threshold photoelectron spectrum of BF was recorded, which leads to an IE of 11.11 eV and an improved value for ν_{BF}^+ of 1690 cm^{-1}. All spectra were simulated by calculating Franck-Condon factors from optimised structures based on quantum chemical calculations.

A Introduction

Boron-containing reactive species such as B-X (borylenes) and X-B-Y appear as intermediates in a variety of applications, including chemical vapor deposition (CVD) of boron carbide and nitride,[1, 2] production of boron-containing films,[3] and doping of semiconductors.[4] Furthermore, boron compounds are of fundamental interest in inorganic chemistry, because they are electron-deficient and lack an octet of electrons around the B atom. This led to the discovery of unusual bonding motives as well as unique reactivities.[5] Detailed spectroscopic studies on reactive boron compounds, which improve our knowledge on the bonding of these species and can aid in their detection in reactive environments, are still scarce. In the present work, we report mass-selected photoelectron spectra of the free radical BH_2, and the two borylenes B-H and B-F, using synchrotron radiation and double imaging photoelectron/photoion coincidence (i²PEPICO) spectroscopy.[6] The spectra are also simulated with the aid of quantum chemical calculations. All species were generated via H-abstraction from B_2H_6 by fluorine atoms created in a microwave discharge. The combination of this technique with photoionization was pioneered by Dyke and coworkers[7-9] and by Ruscic and Berkowitz[10-12]. The latter also recorded first photoionisation mass spectra of B_xH_y compounds.[12, 13] In the present experiments, due to the photoion mass-selection in PEPICO, mass-selected slow photoelectron spectra (ms-SPES) as well as threshold photoelectron spectra (ms-TPES) are recorded. They are not perturbed by possible side products, in contrast to conventional photoelectron spectroscopy and permit to study reactive species ranging from carbon-containing free radicals[14-20] to carbenes,[21] biradicals[22-25] and reactive boron compounds.[24, 26, 27] In recent years PEPICO has also evolved as a reliable analytical tool to detect elusive intermediates in reactive environments such as model flames[28], catalytic reactors[29] or in kinetic experiments.[30, 31]

In its ground electronic state (X^2A_1) BH_2 is a bent, near prolate asymmetric top (C_{2v}) with bond angle ~129°, while in the first excited state ($A^2\Pi_u$) it is linear ($D_{\infty h}$) with slightly shorter B-H bonds.[32-34] With only seven electrons, BH_2 is an attractive system for high-level calculations and hence there are numerous reports on the potential energy surfaces, including rovibronic constants and predictions of the energy barrier to linearity.[33-37] In the first spectroscopic study of BH_2, Herzberg and Johns assigned the bands in spectral region between 11500 cm^{-1} and 15400 cm^{-1} as 2_0^{7-11} vibronic bending mode transitions.[38] Detailed *ab initio* studies corrected this assignment and predicted the origin to be at 4203.9 cm^{-1}.[33, 37] With Laser-induced fluorescence (LIF) and stimulated emission experiments, Tarroni et al. determined the rovibronic energy levels of BH_2 in both ground and first excited state and computed the potential energy surfaces at the CCSD(T)/aug-cc-pV5Z level of theory.[33, 34] In contrast, very few studies deal with the ionization of the molecule. The ionization energy (IE) of BH_2 was first reported by Fehlner and Koski as 9.8 ± 0.2 eV from pyrolysis of diborane, using electron impact mass spectrometry.[39] On the other hand a value of 9.37 eV was

[a] Institute of Physical and Theoretical Chemistry, University of Würzburg, Am Hubland, D-97074 Würzburg, Germany; E-Mail: ingo.fischer@uni-wuerzburg.de
[b] ISM-CNRS, Université de Bordeaux, 351 cours de la Libération, F-33405 Talence, France.
[c] LCP, UMR 8000, CNRS-Univ. Paris-Sud and Paris Saclay, Bât. 350, Centre Universitaire Paris-Sud, F-91405 Orsay, France.
[d] Synchrotron SOLEIL, L'Orme des Merisiers, St Aubin, B.P. 48, F-91192 Gif sur Yvette, France
† Footnotes relating to the title and/or authors should appear here.
Electronic Supplementary Information (ESI) available: [details of any supplementary information available should be included here]. See DOI: 10.1039/x0xx00000x

indirectly extracted from mass spectra.[40] Curtiss and Pople calculated a linear geometry for the cation and predicted an IE of 8.18 eV as well as vibrational frequencies of BH_2^+.[41] However, no vibrationally resolved spectra have been reported for BH_2^+, although the molecule is a textbook case for molecular orbital theory.

Compared to BH_2, the two borylenes BH and BF have been experimentally studied in more detail.[42-61] BH has a singlet electronic ground state, ($X\ ^1\Sigma^+$) with a vibrational wavenumber of 2366.73 cm^{-1}.[62] Fernando and Bernath determined the 0_0^0 transition between ground and first excited singlet state at 23073.97 cm^{-1} and observed a lower vibrational wavenumber of 2251.46 cm^{-1} in the corresponding S_1 state.[53] The rotationally resolved emission spectrum between the two lowest triplet states ($b^3\Sigma^- \rightarrow a^3\Pi$) of BH was measured by Brazier, who reported an energy difference between these two states of 27059.3 cm^{-1} and a B-H bond length elongation of ~0.03 Å in the b-state.[55] The IE of singlet BH was determined as 79120.3 cm^{-1} (9.81033 eV) by Grant and co-workers via Rydberg extrapolation and the value of ω_e^+ was determined as 2526.58 cm^{-1}.[57] Brazier also estimated a singlet-triplet gap ΔE_{ST} of 10410 $\pm$ 300 cm^{-1} by predicting dissociation limits of both states from extrapolated potential energy curves, calculated from experimentally observed spectra,[55] but no direct experimental values of ΔE_{ST} are available.

In the case of BF, apart from the ground ($X^1\Sigma^+$) and first excited singlet ($A^1\Pi$) and triplet ($a^3\Pi$) states, all higher electronic states are Rydberg-type.[59, 61] The $A^1\Pi$ state is located 51088.66 cm^{-1} above the ground state,[45, 59] while the ΔE_{ST} is reported to be 29105.8 cm^{-1}.[48] For BF^+, Canton and Douglas determined an IE of 11.115±0.004 eV and a vibrational wavenumber of 1680 cm^{-1} by Rydberg extrapolation.[45] The IE value was close to the one measured by Hildenbrand (11.06 $\pm$ 0.1 eV) using electron impact mass spectrometry.[46] Dyke et.al reported an IE of 11.12 $\pm$ 0.01 eV and determined ν^+ as 1765 $\pm$ 20 cm^{-1} from the observed vibrational progression in the PES.[49] The authors also explained the shortening of B-F bond upon ionization by considering the ionic nature and charge separation of the B-F bond. Accurate potential energy curves and spectroscopic constants for both BF and BF^+ have been reported using high-level theory, including multireference variational and single reference coupled-cluster method.[59]

B1 Experimental

Experiments were carried out using the DELICIOUS 3 double-imaging photoelectron/ photoion coincidence (i^2PEPICO) spectrometer of the DESIRS VUV undulator beamline located at the French national synchrotron radiation facility SOLEIL (Gif-sur-Yvette, France).[63] BH_2, BH, and BF were produced via reactions of B_2H_6 with fluorine atoms generated in a microwave discharge of F_2 (~5%) diluted in He. The detailed setup was described elsewhere.[24, 64] In brief, commercially available diluted B_2H_6 (0.5% in Ar) was introduced in a flow reactor through a quartz injector tube, which can slide into the reactor tube. The generated F atoms were fed through a side arm attached directly with the reactor. All gas flows were controlled by mass flow controllers and the pressure inside the reactor tube was 0.7-0.8 mbar. Inside the flow tube, F atoms abstract H from B_2H_6 and produce a variety of reaction products, which were subsequently analysed in the attached PEPICO spectrometer. The driving force for the H-abstraction is the large heat of formation of the reaction product, HF ($\Delta_f H°$= -273.3 kJ mol^{-1}).[65] After leaving the reactor, the gas mixture was expanded through a 1 mm Teflon skimmer into a differentially pumped chamber (few 10^{-4} mbar), and through a second skimmer (f = 1 mm) into the ionization chamber ($p \approx 10^{-8}$ mbar). Synchrotron radiation with a narrow bandwidth was selected by a 6.65 m normal incidence monochromator with a 200 g/mm SiC grating and focused onto a 200/200 µm (H/V) spot at the ionization region. The entrance and exit slits were set for a resolution of around 5 meV at the working energy range. A gas filter filled with 0.25 mbar Ar cut off the higher-order radiation from the undulator ensuring spectral purity. The wavelength was calibrated using the atomic lines of Kr and the IE of atomic B. The photon energy was scanned in 5 meV steps, and the data were accumulated for 180-240 s at each point, depending upon the signal intensity of the species of interest. Threshold photoelectron spectra were obtained by selecting electrons with a kinetic energy of up to 10 meV. A slow photoelectron spectrum (SPES) was obtained from the full 2D map (electron kinetic energy vs. photon energy) by the procedure described in reference [66]. Electrons with kinetic energies of up to 50 meV leading to the same final ionic state were included in the SPES. While the resolution is slightly lower compared to TPES, SPES often offers a superior signal/noise ratio, hence is preferable for small signals.

B2 Theoretical

Geometry optimizations followed by calculations of harmonic frequencies in both neutral and cationic states were performed at the CBS-QB3 composite level using the Gaussian 09 program package.[67] Adiabatic ionization energies (IE) were calculated from the differences between the computed zero-point energies of the neutral and cation. Photoelectron spectra were simulated by calculating Franck-Condon (FC) factors between optimized structures using the PGOPHER program, which includes Duschinsky rotation.[68] Although the generated species were thermally not fully equilibrated as will be discussed below, simulations were performed assuming a vibrational temperature of 300 K, which yielded the best match with the experimental spectra. Calculated stick spectra are convoluted by Gaussian functions with a full width at half maximum (FWHM) of 0.025 eV.

C Results and discussion

Mass Spectra

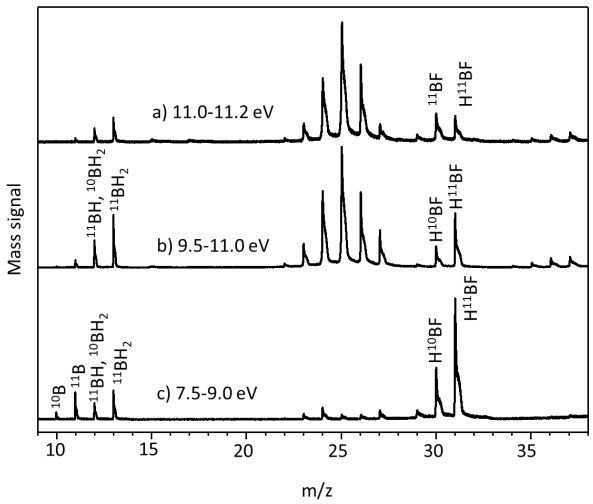

Fig. 1 Normalized mass spectra integrated over the photon energy range specified at each trace, are indicative about the species present in the reactor. The apparent ambiguities in the assignment of the mass peaks can be resolved by considering the 4:1 relative abundance ratio of ^{11}B and ^{10}B isotopes.

Figure 1 depicts the mass spectra integrated over three different photon energy ranges. The different mass peaks indicate reactive intermediates, which were generated in the reactor tube and ionisable in the specified energy range. The abstraction of different numbers of H atoms from the precursor B_2H_6 by F atoms leads to the formation of various B_xH_y species along with BF and HBF. Two isotopes of B (^{11}B and ^{10}B) with a relative abundance of 4:1 make the spectra apparently congested, but the predictable intensity ratio aids in the spectral assignments. Mass peaks around 11 and 25 amu are mainly due to atomic boron, BH_y and B_2H_y type of species. The peaks at 30 and 31 amu result from ^{11}BF, H^{10}BF, and H^{11}BF. The mass spectrum in the bottom trace c) indicates that HBF is the dominant species in this energy range. In traces a) and b), the mass peaks mainly arise from B_2H_y species. The SPES spectrum of the most prominent one, the biradical diborene has been reported recently.[24] Due to its IE of 11.12 eV, BF is only present at the highest photon energies, *cf.* trace a). There are some apparent ambiguities present for assigning the mass peaks at 11, 12 and 30 amu as there are always two possibilities for the carrier of the masses. For example, ^{11}B has m/z = 11 amu, like ^{10}BH. Similarly, ^{11}BH, $^{10}BH_2$, and H^{10}BF, ^{11}BF have m/z values of 12 and 30 amu, respectively. By considering the relative abundance of two boron isotopes, the contributions of the various species can be disentangled. For example, in trace a) the peak at 30 amu likely arises from B^{11}F rather than HB^{10}F, otherwise, the peak at 31 amu is expected to be four times higher than the one at 30 amu.

Photoelectron spectra

The coupled i^{2}PEPICO spectrometer allows us to record the photoelectron spectra of the various species generated inside the reactor with mass selectivity, therefore in the next sections several photoelectron spectra will be discussed. For HBF, the most intense peak in the mass spectrum at low photon energies, both ion and electron signal showed a slow rise. Due to large geometry change upon photoionization, no structured photoelectron spectrum was obtained. Note that for HBBH a SPES has already been reported.[24]

SPES of BH_2. The slow photoelectron spectrum (SPES) recorded for $^{11}BH_2$ is depicted in trace a) of Figure 2. The spectrum is dominated by a progression of 970 cm^{-1}, starting from 8.24 eV, indicating a large geometry change due to photoionization. Employing MO theory as well as a Walsh diagram, BH_2 in its neutral ground state is a bent (C_{2v}) radical (X^2A_1) with a non-bonding electron in an A_1 orbital, while the cationic state is a linear ($D_{\infty h}$) singlet ($^1\Sigma_g^+$).[69] Therefore a large change in the bending angle is expected and the long progression can be assigned as a 2_0^n progression of the bending mode. Geometry optimisation shows that the ground state of neutral BH_2 has a bond angle of 129°, while the singlet cation is linear. Our computations predict a harmonic wavenumber of the bending mode in the cation of 1012 cm^{-1} which does not differ considerably from the computed neutral ground state value of 985 cm^{-1}. However, the B-H bond length (r_{BH}) is lowered by 0.013 Å upon ionization (Table 1). For the linear A-state ($A^2\Pi_u$) of neutral BH_2 a value of 955 cm^{-1} was determined for the bending mode.[38] The similar values for A-state and cation are consistent because an electron in an A_1 type orbital is involved in both cases, i.e. ionization and excitation. The simulated spectra of BH_2 are depicted in the lower two traces of Figure 2. All parameters employed in the simulations are summarised in Table 1. As visible, the simulation is in excellent agreement with the experimentally observed spectrum, deviations become apparent only at higher energy.

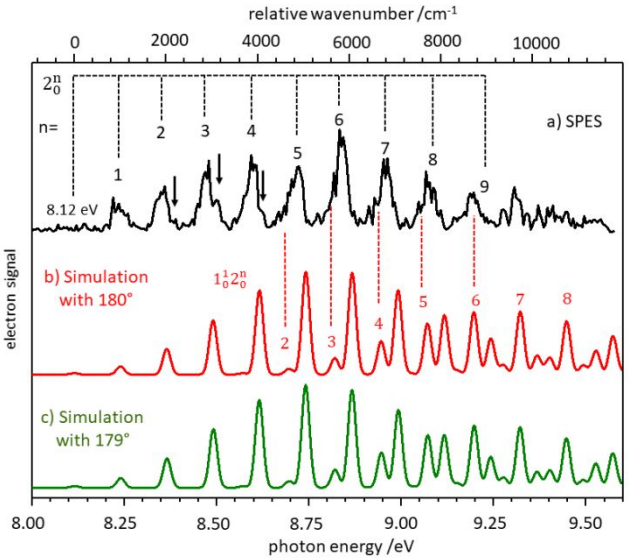

Fig. 2 SPES of $^{11}BH_2$ along with the spectral simulations. Simulated spectra are red shifted by ~0.09 eV to attend the best match with the experimental one. The origin transition, corresponding to the IE is determined as 8.12 eV. The first band in the SPES is assigned as 2_0^1 transition by comparing the band intensities between experiment and simulation.

The predicted adiabatic ionization energies (IE) of $^{11}BH_2$ on the CBS-QB3 and G4 levels of theory are 8.21 and 8.28 eV respectively, consistent with the observed first intense band at 8.24 eV in SPES. However, when the geometry change is large, the first band in the spectrum needs not to coincide with the IE. In fact, the simulation shows negligible intensity for the origin transition and the best match of relative intensities is achieved when the simulated spectra are shifted by 0.09 eV towards lower energy. We, therefore, conclude that the first recognizable peak in the experimental spectrum at 8.24 eV is due to the 2_0^1 fundamental rather than 0_0^0 transition. The origin band is weak due to the small overlap between two significantly displaced ground state vibrational wave functions and is hardly recognizable in the spectrum. Hence, the IE of $^{11}BH_2$ is extracted at 8.12 ± 0.02 eV. The error bars are estimated from the full width at half maximum (FWHM) of the bands. With increasing wavenumber, particularly above +5800 cm^{-1} (0.72 eV) the origin, combination bands of the bending mode progression with one quantum of the symmetric stretching mode ($1_1^1 2_0^n$) become apparent (red dotted lines). Since these bands overlap with the 2_0^n progression, they are difficult to separate in the spectrum. Assignment of those bands in the SPES led to an estimated wave number of the symmetric stretch of $\nu_1^+ = 2680$ cm^{-1}, very close to the CBS-QB3 value of 2664 cm^{-1}. In addition, small features indicated by arrows in Figure 2 at 2130, 3090 and 4060 cm^{-1} seem to appear in the SPES, separated by around 960 cm^{-1} and displaced from the corresponding 2_0^n transition by ≈200 cm^{-1}. By comparison with the computed wavenumbers they can be tentatively assigned as the $2_0^n 3_1^1$ (n=2-4) series of combination bands involving a sequence band of the ν_3^+ asymmetric stretch. To populate the 3_1 level (2739 cm^{-1}) a non-Boltzmann type population distribution is required. Below we will present evidence that such deviation from Boltzmann behaviour does occur in our study.

The different number of vibrational degrees of freedom is a general challenge in computing FC factors for bent to linear transitions. Due to geometric linearization in the cationic state, an extra vibrational degree of freedom arises in expense of one lost rotational degree of freedom and the bending vibration becomes degenerate. Almost all programs which can calculate FC factors for polyatomic molecules use Duschinsky rotation.[70] In this scheme, the normal modes of two electronic states (Q″Q′) are related by the following equation.

$$Q' = JQ'' + K \qquad (1)$$

Here K represents the change in equilibrium geometry and J accounts for mixing between modes. Q″ and Q′ are two column matrices of normal coordinates with the dimensions (3N-6) or (3N-5) depending on the geometry. N is the number of atoms in the molecule and the J matrix is a square transformation matrix. If Q″ and Q′ have a different dimension, then the scheme fails as J can no longer be a square matrix. To maintain the same number of normal modes in both cation and neutral, two approaches have been used here.

Species	El. State	Experiment		Theory (CBS-QB3), this work			
		IE_{ad} /eV	ν /cm^{-1}	IE_{ad} /eV	ν /cm^{-1}	r /Å	Bond angle
$^{11}BH_2$	X $^2A_1$	8.12	2509[a] 974[a] -	8.21	2573 985 2739	1.188	129°
$^{11}BH_2^+$	X $^1\Sigma_g^+$	-	2680 970 -		2664 1012 1012 2953	1.175	180°
^{11}BH	X $^1\Sigma^+$	9.82	2367[b]	9.84	2331	1.237	
	a $^3\Pi$	8.48	2625[c]	8.42	2605	1.193	
$^{11}BH^+$	X $^2\Sigma^+$	-	2370		2531	1.205	
^{11}BF	X $^1\Sigma^+$	11.11	1410	11.19	1381	1.267	
$^{11}BF^+$	X $^2\Sigma^+$	-	1690		1668	1.216	

Table 1 Comparison of experimentally determined and theoretically predicted parameters of $^{11}BH_2$, ^{11}BH and ^{11}BF.

a) ref [34], b) ref [53], c) ref [55]

In the first approach, only one of the two bending components was considered in the cation. In the second approach, a slightly nonlinear geometry with a bond angle of 179° instead of 180° in the cation was employed in the simulations. It is worth mentioning that the partially optimized structure with a bond angle of 179° is very similar compared to the fully optimized one. The electronic energies of these two structures of the cation differ only by 0.3 meV and the bond lengths differ by only 0.0004 Å. Simulated spectra in PGOPHER considering both approaches are depicted in red and green along with the experimentally observed spectrum in Figure 2. As expected, the results are very similar and agree well with the experiment. It is important to note that in the first scheme the choice of the bending mode component leads to different simulated spectra and only one is consistent with the observations. A simulation based on the second component of the bending vibration is illustrated in the supplementary information (Figure S1). A rigorous calculation of full-dimensional FC factors for this bent-to-linear transition requires inclusion of correlations between vibrational angular momentum of the linear state with rotations of the bent state.[71, 72] Given the excellent agreement of our simulations with the experimental spectrum, we are convinced such an expensive calculation can be avoided for the present system.

BH. The SPES of ^{11}BH is illustrated in Figure 3. The most intense band at 9.82 ±0.02 eV is assigned as the BH^+ ($X\ ^2\Sigma^+$) ← BH ($X\ ^1\Sigma^+$)

origin transition in agreement with computations (9.84 eV) as well as the experimental IE of 79,120.3 cm^{-1} (9.81033 eV) reported for singlet BH from a Rydberg extrapolation.[57] A short progression results from the slight decrease of r_{BH} upon ionization and the bands appearing at +2370 cm^{-1} and +4500 cm^{-1} are assigned to the fundamental and first overtone respectively. Although the progression is too short to analyse the anharmonicity of the potential in detail, the data are consistent with the vibrational constant ω_e^+ = 2526.58 cm^{-1} reported earlier.[57] The simulated spectrum in the lower trace also agrees well with the experiment.

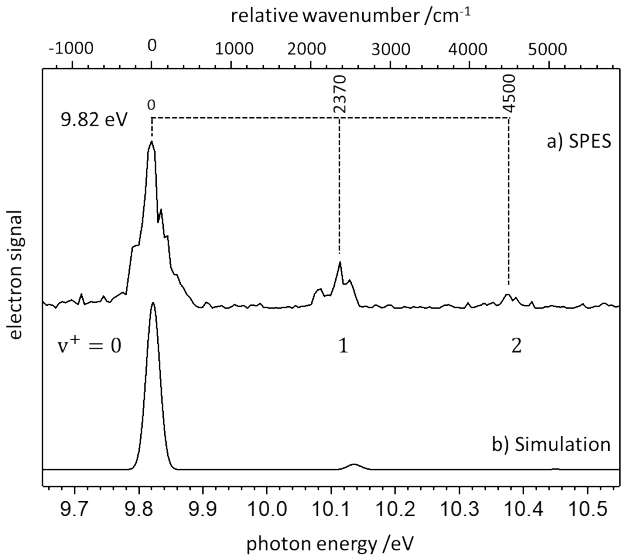

Fig. 3 Normalized SPES of ^{11}BH from the X $^1\Sigma^+$ state and the corresponding simulated spectrum. The latter is red shifted by 0.02 eV to match the measured SPES. The upper abscissa scale indicates the relative shift of wavenumber from origin transition.

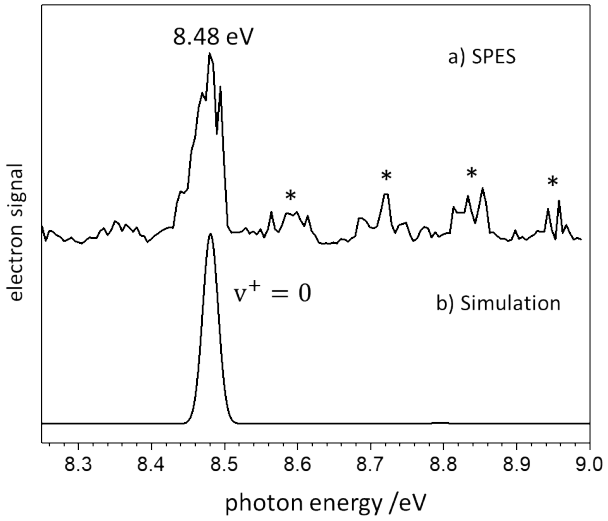

Fig. 4 Normalized SPES of ^{11}BH from the *a* $^3\Pi$ state and the corresponding simulation in PGOPHER. The simulated spectrum is blue shifted by 0.06 eV to match the band position with SPES. Bands marked with asterisks are due to the $^{10}BH_2$ which has the same mass with the ^{11}BH.

At lower photon energies a further band appears at 8.48 eV in the m/z=12 mass channel, see Figure 4. While several other small features marked by asterisks can be assigned to $^{10}BH_2$ by comparison with the spectrum given in Figure 2, this peak has no counterpart in the m/z=13 channel and thus must be assigned to ^{11}BH. We, therefore, assign this band to the BH^+ (X $^2\Sigma^+$) ← BH (a $^3\Pi$) transition and conclude that the band at 8.48 ± 0.02 eV corresponds to the adiabatic IE of triplet BH. This is in very good agreement with the computed IE of 8.43 eV. Few data are available for the triplet state of BH.[55, 73] From the IE's of singlet and triplet BH, we determined ΔE_{ST} to be 1.34±0.03 eV, equivalent to 10808±200 cm^{-1}. Combining our value for triplet BH with the more accurate IE for the singlet derived via Rydberg extrapolation[57] leads to ΔE_{ST} =10730±160 cm^{-1}. Brazier estimated ΔE_{ST} =10410 ± 300 cm^{-1} from the potential energy curves obtained by fitting experimentally observed vibrational frequencies,[55] while Mavridis et al computed ΔE_{ST} =10588 cm^{-1} using multi-reference configuration interaction (MRCI).[73] To the best of our knowledge, the present work leads to the first direct experimentally determined value for ΔE_{ST} of BH. Neither experiment nor the simulations show evidence for vibrational activity, consistent with the small increase of r_{BH} by only 0.012 Å upon photoionization from the $a^3\Pi$ state. In contrast, r_{BH} decreases by 0.032 Å in the photoionization of the X $^1\Sigma^+$ state. Furthermore, the predicted vibrational wavenumber changes by only 74 cm^{-1} between triplet and cation, whereas for the singlet state this difference is 200 cm^{-1}. This can be explained by the valence-bond-Lewis (vbL) diagram of the BH described by Mavridis et.al.[73] The *s*-character of the B-H σ-bond increases due to *sp*-hybridization of the B atom while going from singlet to triplet state.

The observation of triplet BH in the experiment is a striking example of the non-equilibrium conditions in the fluorine reactor. In the stepwise abstraction of hydrogen atoms, BH is formed from B_2H_6 in both singlet and triplet state. Obviously, the number of spin-changing collisions is too small to equilibrate the electronic population of BH and the lifetime of the *a* $^3\Pi$ state is sufficiently long to be detected. In contrast, the translational and rotational degrees of freedom are cooled efficiently due to the much higher efficiency of energy transfer in collisions. In previous experiments on NH_2, rotations were cooled more efficiently in the fluorine reactor than in a pyrolysis source and temperatures between 170 K and 300 K were achieved.[74]

BF. Figure 5 shows the TPE spectrum of B-F. The first intense band at 11.11 eV has been assigned to the origin of the BF^+ (X $^2\Sigma^+$) ← BF (X $^1\Sigma^+$) transition, corresponding to the IE of BF, a value that is consistent with previous experimental reports.[46, 49] The main feature observed in this spectrum is a vibrational progression of 1690 cm^{-1} that can be followed up to the second overtone.

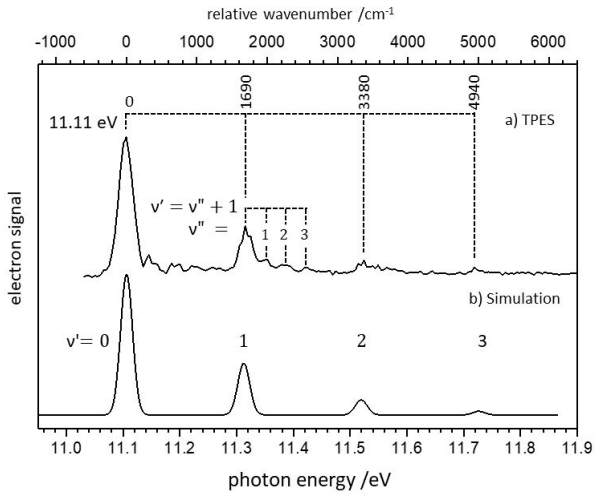

Figure 5 Normalized TPES of ^{11}BF and the corresponding spectral simulation. The simulated spectrum is red shifted by 0.08 eV to attend the best match with the recorded spectrum. Though the sequence bands are also visible at the origin transition, they are more pronounced close to the $v^+ = 1$ band and easy to assign.

The relative intensities of the members of this progression are similar to the 1765 cm^{-1} progression reported by Dyke *et al*.[49] Figure 5 also shows that the spectrum simulated in PGOPHER is in good agreement with the measured spectrum. Vibrational wavenumbers computed on the CBS-QB3 level (1668 cm^{-1}) as well as on a higher level of theory[59] including MRCI (1700 cm^{-1}) and RCCSD(T) (1699 cm^{-1}) agree well with our observation. Bands, which are accompanied by smaller features on the high-energy side with a spacing of around 280 cm^{-1}, can be assigned as sequence band transitions. The sequence bands appear with very low intensity in the depicted spectrum but are clearly discernible. From the sequence band progression we derive a vibrational wavenumber of 1410 cm^{-1} for BF, consistent with ω_e =1402.2 cm^{-1} as reported by Zhang et al.[54] The unusually high population of vibrational levels up to v"=3 again confirms a non-equilibrium vibrational population of the intermediates formed in the reactor. As mentioned above, BF is formed after a sequence of H-abstraction steps with excess vibrational energy that is not released in the subsequent subsonic expansion. For example, in recent experiments on CNN, isomerisation to CNC was observed, despite the barrier of around 2 eV.[75] Therefore, sequence transitions are expected to be apparent for the species generated in the present reactor.

One would expect also the appearance of hot bands in the TPES of BF. However, the v"=1 $\rightarrow$ v$^+$=0 transition will appear outside the investigated scan range and the v"=2 $\rightarrow$ v$^+$=1 transition most likely overlaps with the v$^+$=v sequence bands that accompany the origin transition.

Conclusions

Mass-selected photoelectron spectra of three Boron containing reactive species, BH_2, BH, and BF were recorded using synchrotron radiation coupled with an i^{2}PEPICO spectrometer. All species were generated in a flow-tube reactor from B_2H_6 using fluorine atoms produced in a F_2 microwave discharge. The spectrum of BH_2 shows a bending mode progression up to the 9th overtone due to linearization upon photoionization. By comparing simulated and experimental spectra the IE of BH_2 was determined to be 8.12±0.02 eV, although the origin transition occurs with negligible intensity, and the wavenumber of the bending modes as 970 cm^{-1}. A value of 2680 cm^{-1} was also tentatively derived for the ν_1 symmetric stretching mode of $\mathbf{BH_2^+}$. For BH, photoionisation from both $X^1\Sigma^+$ singlet and $a^3\Pi$ triplet state was observed, yielding IE's of 9.82 eV and 8.48 eV respectively, which also permit the experimental determination of singlet/triplet gap (ΔE_{ST}). From the difference between our value for the $a^3\Pi$ state and the IE for the $X^1\Sigma^+$ state derived by Rydberg extrapolation, ΔE_{ST} of BH was determined to be 1.33±0.02 eV (10.730 cm^{-1}), which agrees well with computations and earlier estimates. The TPES of BF shows a short vibrational progression of 1690 cm^{-1} followed by some sequence transitions. As in previous works on radicals obtained by H abstraction the exothermicity of the reaction leads to non-Boltzmann populations of the vibrational and electronic degrees of freedom. The reaction products of each H-abstraction step take up a fraction of the released heat, but unlike in a supersonic expansion the small number of collisions in the effusive molecular beam is insufficient to cool the molecules to the vibrational ground state, hence higher vibrational levels and even excited electronic states are populated.

Acknowledgements

This work was performed on the DESIRS beamline under Proposal No. 20180287. We acknowledge SOLEIL for provision of synchrotron radiation facilities and the DESIRS beamline team for their assistance. The work was financially supported by the Deutsche Forschungsgemeinschaft, Fi 575/13-1, and the Agence Nationale de la Recherche (ANR) under grant number ANR-12- BS08-0020-02 (project SYNCHROKIN).

Notes and references

1. A. O. Sezer and J. I. Brand, *Mat. Sci. Eng. B*, 2001, **79**, 191-202.
2. G. Reinisch, S. Patel, G. Chollon, J. M. Leyssale, D. Alotta, N. Bertrand and G. L. Vignoles, *J. Nanosci. Nanotechnol.*, 2011, **11**, 8323-8327.
3. W. Gajewski, P. Achatz, O. A. Williams, K. Haenen, E. Bustarret, M. Stutzmann and J. A. Garrido, *Phys. Rev. B*, 2009, **79**.
4. J. Xu, M. C. Granger, Q. Chen, J. W. Strojek, T. E. Lister and G. M. Swain, *Anal. Chem.*, 1997, **69**, 591A-597A.

5. M. A. Legare, M. Rang, G. Belanger-Chabot, J. I. Schweizer, I. Krummenacher, R. Bertermann, M. Arrowsmith, M. C. Holthausen and H. Braunschweig, *Science*, 2019, **363**, 1329-1332.
6. T. Baer and R. P. Tuckett, *Phys Chem Chem Phys*, 2017, **19**, 9698-9723.
7. J. Baker, M. Barnes, M. G. R. Cockett, J. M. Dyke, A. M. Ellis, M. Fehér, E. P. F. Lee, A. Morris and H. Zamanpour, *J. Electron Spectr. Rel. Phenom.*, 1990, **51**, 487-511.
8. J. D. Barr, L. Beeching, A. De Fanis, J. M. Dyke, S. D. Gamblin, N. Hooper, A. Morris, S. Stranges, J. B. West, A. E. Wright and T. G. Wright, *J. Electron Spectr. Rel. Phenom.*, 2000, **108**, 47-61.
9. J. M. Dyke, *Phys Chem Chem Phys*, 2019, **21**, 9106-9136.
10. B. Ruščic, M. Schwarz and J. Berkowitz, *J. Chem. Phys.*, 1989, **91**, 4576-4581.
11. B. Ruscic, *Res. Adv. Phys. Chem*, 2000, **1**, 39-75.
12. J. Berkowitz, *Acc. Chem. Res.*, 2002, **22**, 413-420.
13. B. Ruscic, C. A. Mayhew and J. Berkowitz, *J. Chem. Phys.*, 1988, **88**, 5580-5593.
14. T. Schüßler, H.-J. Deyerl, S. Dümmler, I. Fischer, C. Alcaraz and M. Elhanine, *J. Chem. Phys.*, 2003, **118**, 9077-9080.
15. P. Hemberger, M. Lang, B. Noller, I. Fischer, C. Alcaraz, B. K. Cunha de Miranda, G. A. Garcia and H. Soldi-Lose, *J. Phys. Chem. A*, 2011, **115**, 2225-2230.
16. J. D. Savee, J. Zádor, P. Hemberger, B. Sztáray, A. Bodi and D. L. Osborn, *Mol. Phys.*, 2015, **113**, 2217-2227.
17. B. Gans, G. A. Garcia, F. Holzmeier, J. Kruger, A. Roder, A. Lopes, C. Fittschen, J. C. Loison and C. Alcaraz, *J Chem Phys*, 2017, **146**, 011101.
18. E. Reusch, F. Holzmeier, P. Constantinidis, P. Hemberger and I. Fischer, *Angew. Chem. Int. Ed. Engl.*, 2017, **56**, 8000-8003.
19. L. H. Coudert, B. Gans, G. A. Garcia and J. C. Loison, *J Chem Phys*, 2018, **148**, 054302.
20. K. Voronova, K. M. Ervin, K. G. Torma, P. Hemberger, A. Bodi, T. Gerber, D. L. Osborn and B. Sztaray, *J Phys Chem Lett*, 2018, **9**, 534-539.
21. F. Holzmeier, I. Fischer, B. Kiendl, A. Krueger, A. Bodi and P. Hemberger, *Phys. Chem. Chem. Phys.*, 2016, **18**, 9240-9247.
22. M. Steglich, V. B. F. Custodis, A. J. Trevitt, G. daSilva, A. Bodi and P. Hemberger, *J Am Chem Soc*, 2017, **139**, 14348-14351.
23. E. Reusch, D. Kaiser, D. Schleier, R. Buschmann, A. Krueger, T. Hermann, B. Engels, I. Fischer and P. Hemberger, *J Phys Chem A*, 2019, **123**, 2008-2017.
24. D. Schleier, A. Humeniuk, E. Reusch, F. Holzmeier, D. Nunez-Reyes, C. Alcaraz, G. A. Garcia, J. C. Loison, I. Fischer and R. Mitric, *J Phys Chem Lett*, 2018, **9**, 5921-5925.
25. D. V. Chicharro, S. M. Poullain, L. Banares, H. R. Hrodmarsson, G. A. Garcia and J. C. Loison, *Phys Chem Chem Phys*, 2019, **21**, 12763-12766.
26. K. H. Fischer, M. Schneider, I. Fischer, B. Pfaffinger, H. Braunschweig, B. Sztaray and A. Bodi, *Chem. Eur. J.*, 2012, **18**, 4533-4540.
27. F. Holzmeier, M. Lang, P. Hemberger, A. Bodi, M. Schafer, R. D. Dewhurst, H. Braunschweig and I. Fischer, *Chem. Eur. J.*, 2014, **20**, 9683-9692.
28. J. Kruger, G. A. Garcia, D. Felsmann, K. Moshammer, A. Lackner, A. Brockhinke, L. Nahon and K. Kohse-Hoinghaus, *Phys Chem Chem Phys*, 2014, **16**, 22791-22804.
29. P. Hemberger, V. B. F. Custodis, A. Bodi, T. Gerber and J. A. van Bokhoven, *Nature Comm.*, 2017, **8**, 15946.
30. B. Sztaray, K. Voronova, K. G. Torma, K. J. Covert, A. Bodi, P. Hemberger, T. Gerber and D. L. Osborn, *J Chem Phys*, 2017, **147**, 013944.
31. D. Schleier, P. Constantinidis, N. Fassheber, I. Fischer, G. Friedrichs, P. Hemberger, E. Reusch, B. Sztaray and K. Voronova, *Phys Chem Chem Phys*, 2018, **20**, 10721-10731.
32. G. Herzberg, *Molecular spectra and molecular structure*, Van Nostrand, 1966.
33. F. X. Sunahori, M. Gharaibeh, D. J. Clouthier and R. Tarroni, *J Chem Phys*, 2015, **142**, 174302.
34. B. Jin, D. J. Clouthier and R. Tarroni, *J Chem Phys*, 2017, **147**, 124303.
35. M. Perić, S. D. Peyerimhoff and R. J. Buenker, *Can. J. Chem.*, 1981, **59**, 1318-1327.
36. M. Brommer, P. Rosmus, S. Carter and N. Handy, *Mol. Phys.*, 1992, **77**, 549-561.
37. M. Kolbuszewski, *Mol. Phys.*, 1996, **88**, 105-124.
38. G. Herzberg and J. W. C. Johns, *Proc. Royal Soc. A* 1967, **298**, 142-159.
39. T. P. Fehlner and W. S. Koski, *J. Am. Chem. Soc.*, 1964, **86**, 2733-2734.
40. J. H. Wilson and H. A. McGee, *J. Chem. Phys.*, 1967, **46**, 1444-1453.
41. L. A. Curtiss and J. A. Pople, *J. Phys. Chem.*, 1988, **92**, 894-899.
42. R. F. Barrow, D. Premaswarup, J. Winternitz and P. B. Zeeman, *Proc. Phys. Soc.*, 1958, **71**, 61-64.
43. D. W. Robinson, *J. Mol. Spectrosc.*, 1963, **11**, 275-300.
44. S. H. Bauer, G. Herzberg and J. W. C. Johns, *J. Mol. Spectrosc.*, 1964, **13**, 256-280.
45. R. B. Caton and A. E. Douglas, *Can. J. Phys.*, 1970, **48**, 432-452.
46. D. L. Hildebrand, *Int. J. Mass Spectrom. Ion Phys.*, 1971, **7**, 255-260.
47. F. J. Lovas and D. R. Johnson, *J. Chem. Phys.*, 1971, **55**, 41-44.
48. J. Lebreton, J. Ferran and L. Marsigny, *J. Phys. B: At. Mol. Opt. Phys.*, 1975, **8**, L465-L466.
49. J. M. Dyke, C. Kirby and A. Morris, *J. Chem. Soc., Faraday Trans. 2*, 1983, **79**, 483-490.
50. W.-T. Luh and W. C. Stwalley, *J. Mol. Spectrosc.*, 1983, **102**, 212-223.
51. O. Gustafsson and M. Rittby, *J. Mol. Spectrosc.*, 1988, **131**, 325-339.
52. F. S. Pianalto, L. C. O'Brien, P. C. Keller and P. F. Bernath, *J. Mol. Spectrosc.*, 1988, **129**, 348-353.
53. W. T. M. L. Fernando and P. F. Bernath, *J. Mol. Spectrosc.*, 1991, **145**, 392-402.
54. K. Q. Zhang, B. Guo, V. Braun, M. Dulick and P. F. Bernath, *J. Mol. Spectrosc.*, 1995, **170**, 82-93.
55. C. R. Brazier, *J. Mol. Spectrosc.*, 1996, **177**, 90-105.
56. J. Clark, M. Konopka, L.-M. Zhang and E. R. Grant, *Chem. Phys. Lett.*, 2001, **340**, 45-54.
57. C. Ricardo Viteri, A. T. Gilkison, S. J. Rixon and E. R. Grant, *J Chem Phys*, 2006, **124**, 144312.
58. C. R. Viteri, A. T. Gilkison, S. J. Rixon and E. R. Grant, *Phys. Rev. A*, 2007, **75**.
59. I. Magoulas, A. Kalemos and A. Mavridis, *J Chem Phys*, 2013, **138**, 104312.
60. J. Koput, *J Comput Chem*, 2015, **36**, 2219-2227.

61. M. Krasowska, M. Edelmann and H. F. Bettinger, *J Phys Chem A*, 2016, **120**, 6332-6341.
62. G. Herzberg, J. W. T. Spinks and K. P. Huber, *Molecular spectra and molecular structure Vol. 4, Vol. 4*, Van Nostrand Reinhold, New York, 1979.
63. G. A. Garcia, B. K. Cunha de Miranda, M. Tia, S. Daly and L. Nahon, *Rev. Sci. Instrum.*, 2013, **84**, 053112.
64. G. A. Garcia, B. Gans, X. Tang, M. Ward, S. Batut, L. Nahon, C. Fittschen and J.-C. Loison, *J. Electron Spectr. Rel. Phenom.*, 2015, **203**, 25-30.
65. J. D. Cox, D. D. Wagman and V. A. Medvedev, *CODATA key values for thermodynamics*, Hemisphere Pub. Corp., New York, 1989.
66. J. C. Poully, J. P. Schermann, N. Nieuwjaer, F. Lecomte, G. Gregoire, C. Desfrancois, G. A. Garcia, L. Nahon, D. Nandi, L. Poisson and M. Hochlaf, *Phys Chem Chem Phys*, 2010, **12**, 3566-3572.
67. M. J. Frisch, G. W. Trucks, H. B. Schlegel, G. E. Scuseria, M. A. Robb, J. R. Cheeseman, G. Scalmani, V. Barone, B. Mennucci, G. A. Petersson, H. Nakatsuji, M. Caricato, X. Li, H. P. Hratchian, A. F. Izmaylov, J. Bloino, G. Zheng, J. L. Sonnenberg, M. Hada, M. Ehara, K. Toyota, R. Fukuda, J. Hasegawa, M. Ishida, T. Nakajima, Y. Honda, O. Kitao, H. Nakai, T. Vreven, J. A. Montgomery, J. E. Peralta, F. Ogliaro, M. Bearpark, J. J. Heyd, E. Brothers, K. N. Kudin, V. N. Staroverov, R. Kobayashi, J. Normand, K. Raghavachari, A. Rendell, J. C. Burant, S. S. Iyengar, J. Tomasi, M. Cossi, N. Rega, J. M. Millam, M. Klene, J. E. Knox, J. B. Cross, V. Bakken, C. Adamo, J. Jaramillo, R. Gomperts, R. E. Stratmann, O. Yazyev, A. J. Austin, R. Cammi, C. Pomelli, J. W. Ochterski, R. L. Martin, K. Morokuma, V. G. Zakrzewski, G. A. Voth, P. Salvador, J. J. Dannenberg, S. Dapprich, A. D. Daniels, Farkas, J. B. Foresman, J. V. Ortiz, J. Cioslowski and D. J. Fox, *Gaussian 09, Revision B.01*, Wallingford CT, 2009.
68. C. M. Western, *JQSRT,* 2017, **186**, 221-242.
69. A. D. Walsh, *J. Chem. Soc. (Resumed)*, 1953, DOI: 10.1039/jr9530002260.
70. F. Duschinsky, *Acta Physicochim. URSS*, 1937, **7**, 441.
71. G. B. Park, *J. Chem. Phys.*, 2014, **141**, 134304.
72. G. B. Park, J. H. Baraban and R. W. Field, *J. Chem. Phys.*, 2014, **141**, 134305.
73. E. Miliordos and A. Mavridis, *J Chem Phys*, 2008, **128**, 144308.
74. F. Holzmeier, M. Lang, I. Fischer, P. Hemberger, G. A. Garcia, X. Tang and J. C. Loison, *Phys Chem Chem Phys*, 2015, **17**, 19507-19514.
75. G. A. Garcia, J. Kruger, B. Gans, C. Falvo, L. H. Coudert and J. C. Loison, *J Chem Phys*, 2017, **147**, 013908.

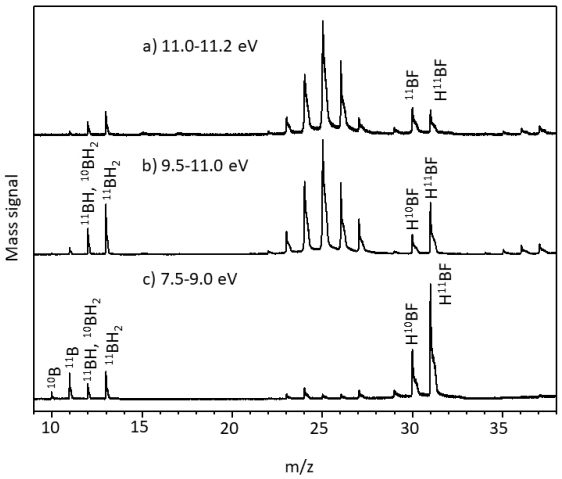

Fig. 1 Normalized mass spectra integrated over the photon energy range specified at each trace, are indicative about the species present in the reactor. The apparent ambiguities in the assignment of the mass peaks can be resolved by considering the 4:1 relative abundance ratio of 11B and 10B isotopes.

338x190mm (96 x 96 DPI)

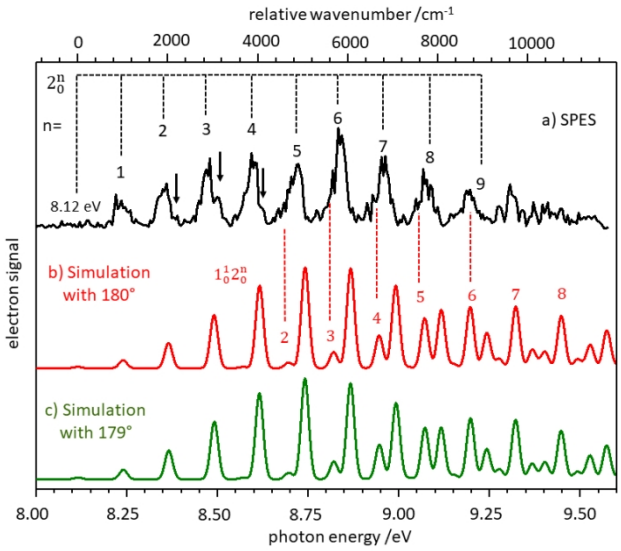

Fig. 2 SPES of 11BH2 along with the spectral simulations. Simulated spectra are shifted by ~0.09 eV to lower energy to attend the best match with the experimental one. The origin transition, corresponding to the IE is determined as 8.12 eV. The first band in the SPES is assigned as 2_0^1 transition by comparing the band intensities between experiment and simulation.

338x190mm (96 x 96 DPI)

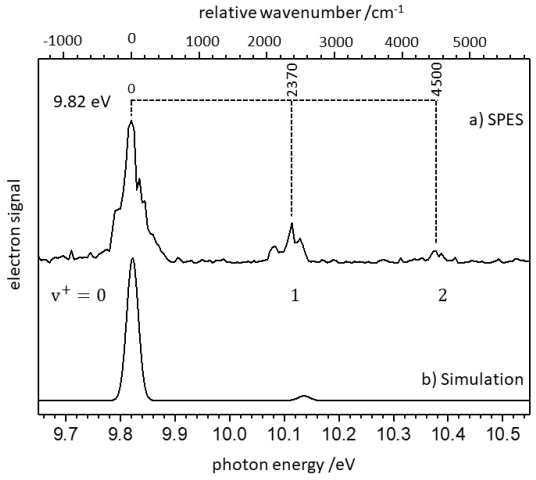

Fig. 3 Normalized SPES of 11BH from the X 1Σ+ state and the corresponding simulated spectrum. The latter is shifted to lower energy by 0.02 eV to match the measured SPES. The upper abscissa scale indicates the relative shift of wavenumber from origin transition.

338x190mm (96 x 96 DPI)

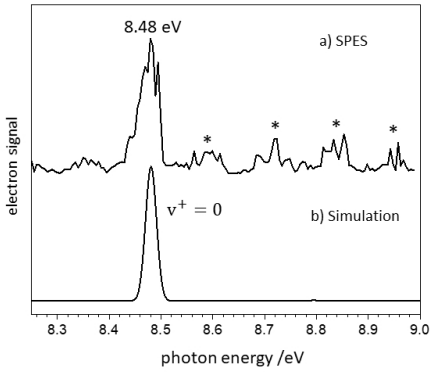

Fig. 4 Normalized SPES of 11BH from the a 3Π state and the corresponding simulation in PGOPHER. The simulated spectrum is shifted to higher energy by 0.06 eV to match the band position with SPES. Bands marked with asterisks are due to the 10BH2 which has the same mass with the 11BH.

338x190mm (96 x 96 DPI)

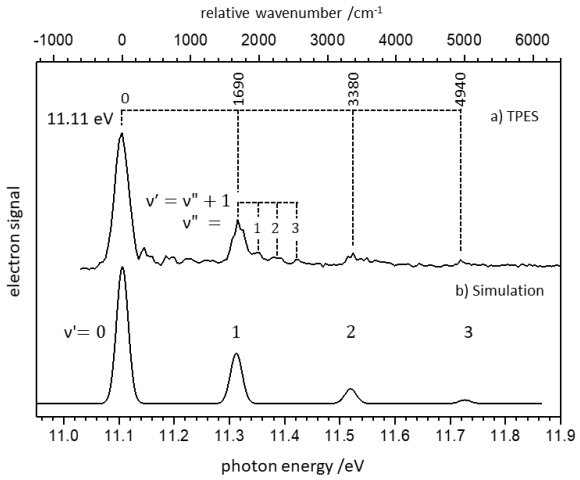

Figure 5 Normalized TPES of 11BF and the corresponding spectral simulation. The simulated spectrum is red shifted by 0.08 eV to attend the best match with the recorded spectrum. Though the sequence bands are also visible at the origin transition, they are more pronounced close to the v^+=1 band and easy to assign.

338x190mm (96 x 96 DPI)

Electronic Supplementary information to

Photoelectron spectroscopy of boron-containing reactive intermediates using synchrotron radiation: BH_2, BH, and BF

D.P. Mukhopadhyay,[a] D. Schleier, [a] I. Fischer [a] ,*J.-C. Loison,[b] C. Alcaraz,[c] and G. A. Garcia[d]

a. Institute of Physical and Theoretical Chemistry, University of Würzburg, Am Hubland, D-97074 Würzburg, Germany; E-Mail: ingo.fischer@uni-wuerzburg.de

b. ISM-CNRS, Université de Bordeaux, 351 cours de la Libération, F-33405 Talence, France.

c. LCP, UMR 8000, CNRS-Univ. Paris-Sud and Paris Saclay, Bât. 350, Centre Universitaire Paris-Sud, F-91405 Orsay, France.

d. Synchrotron SOLEIL, L'Orme des Merisiers, St Aubin, B.P. 48, F-91192 Gif sur Yvette, France

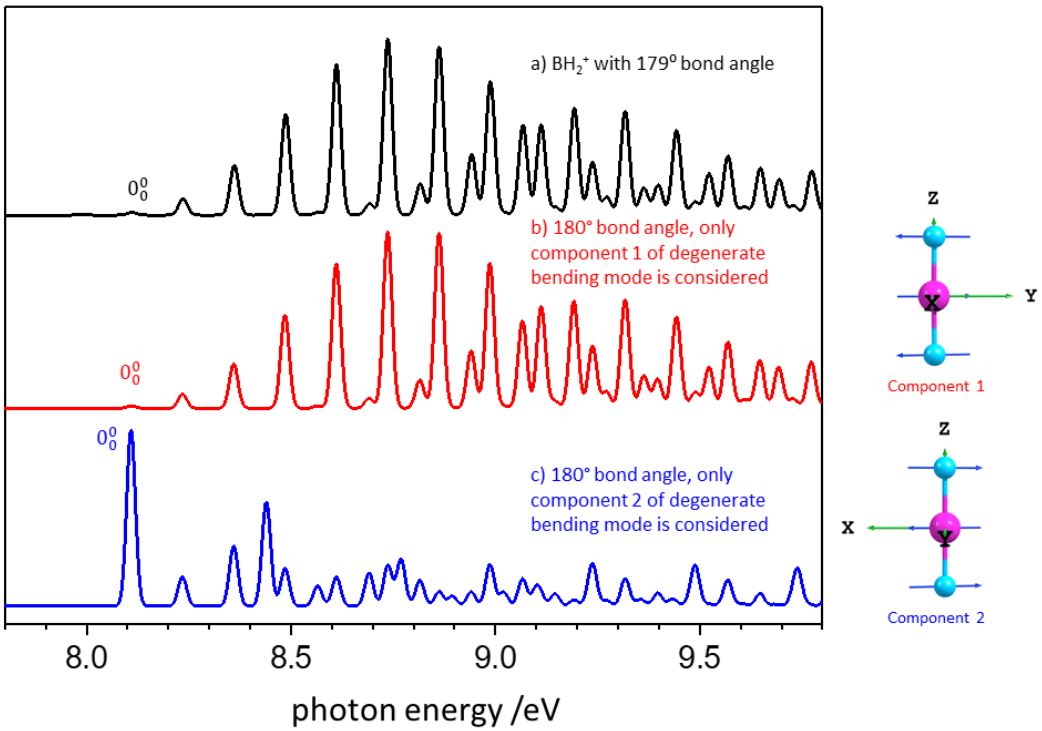

Figure S1: Comparison of different simulations of the slow photoelectron spectrum (SPES) of $^{11}BH_2$, using PGOPHER.[1] Trace a) assumes a cationic geometry with 179^0 bond angle. Trace b) and c) correspond to the linear cation, considering only the component of the bending vibration indicated on the right-hand side of the Figure. The z-axis is chosen as the principal axis. It is evident that simulations a) and b) are consistent with the experimental spectrum, while the simulation given in trace c) is inconsistent.

1. C. M. Western, *JQSRT*, 2017, **186**, 221-242.